Two-photon high-resolution measurement of partial pressure of oxygen in cerebral vasculature and tissue

Sava Sakadžić[1], Emmanuel Roussakis[2], Mohammad A Yaseen[1], Emiri T Mandeville[3], Vivek J Srinivasan[1], Ken Arai[3], Svetlana Ruvinskaya[1], Anna Devor[1,4], Eng H Lo[3], Sergei A Vinogradov[2] & David A Boas[1]

Measurements of oxygen partial pressure (pO_2) with high temporal and spatial resolution in three dimensions is crucial for understanding oxygen delivery and consumption in normal and diseased brain. Among existing pO_2 measurement methods, phosphorescence quenching is optimally suited for the task. However, previous attempts to couple phosphorescence with two-photon laser scanning microscopy have faced substantial difficulties because of extremely low two-photon absorption cross-sections of conventional phosphorescent probes. Here we report to our knowledge the first practical *in vivo* two-photon high-resolution pO_2 measurements in small rodents' cortical microvasculature and tissue, made possible by combining an optimized imaging system with a two-photon–enhanced phosphorescent nanoprobe. The method features a measurement depth of up to 250 μm, sub-second temporal resolution and requires low probe concentration. The properties of the probe allowed for direct high-resolution measurement of cortical extravascular (tissue) pO_2, opening many possibilities for functional metabolic brain studies.

The functioning of the brain is critically dependent on oxygen supply[1–3]. Previous measurements indicate great variability in both vascular and tissue oxygen partial pressure (pO_2)[4–7] that is likely to arise from variations in blood flow and metabolic demand in different regions of the brain. Precise mechanisms of the regulation of the oxygen supply, however, are still largely unknown[8], in part because of an inability to accurately and rapidly measure cortical vascular and tissue pO_2 at increased depth with high resolution. The existing oxygen measurement methods (for example, electrodes[7], binding of nitroimidazole-based drugs[9], electron paramagnetic resonance methods[10,11] and hemoglobin optical absorption–based methods[12–14]) suffer from either low sensitivity or low spatial or temporal resolution, or are invasive. Among optical approaches, oxygen-dependent quenching of phosphorescence[15] stands out in its ability to provide fast absolute measurements of pO_2, which are unaffected by changes in optical properties of the tissue. Previous studies have applied phosphorescence quenching to image oxygen in various biological tissues[16–20], including examples of microscopy[21].

The synergy of phosphorescence quenching with two-photon microscopy[22] is natural because two-photon excitation, which is characterized by a high degree of spatial confinement and a reduced risk of photodamage, should allow pO_2 measurements deeper in the brain with high resolution. Unfortunately, direct coupling of phosphorescence with two-photon microscopy is hampered by extremely low two-photon absorption cross-sections of phosphorescent probes, necessitating very high excitation powers, long acquisition periods and/or exceedingly high probe concentrations[23,24]. Here we show that, by using a specially designed two-photon–enhanced phosphorescent nanoprobe platinum porphyrin–coumarin-343 (PtP-C343) (ref. 25) and an optimized microscopy setup, these limitations can be overcome, allowing for pO_2 measurements in capillaries down to 240 μm below the brain surface with high (~0.5 s per point) temporal resolution. The signal in these measurements is phosphorescence lifetime, not intensity, and thus it is independent of the local probe concentration. We report an extensive map of intravascular pO_2 values as they vary from the pial arteries through the capillary network into the draining veins. Furthermore, the unique properties of the probe allowed for, to our knowledge, the first, direct high-resolution measurements of cortical tissue pO_2 *in vivo* down to 100 μm below the brain surface. We demonstrated the functionality of this method by measuring spatiotemporal variations in tissue pO_2 arising from hypoxia and by simultaneously measuring intravascular and extravascular (tissue) pO_2.

RESULTS

Two-photon–enhanced phosphorescent probe PtP-C343

PtP-C343 (ref. 25) (**Supplementary Fig. 1**), belongs to the family of dendritically protected phosphorescent probes[26]. Its core is formed by a highly phosphorescent Pt porphyrin encapsulated inside poly(arylglycine) dendrimer. The dendrimer protects the porphyrin from interaction with components of the measurement system and controls the rate of oxygen quenching. Several

[1]Photon Migration Imaging Laboratory, Athinoula A. Martinos Center for Biomedical Imaging, Department of Radiology, Massachusetts General Hospital and Harvard Medical School, Charlestown, Massachusetts, USA. [2]Department of Biochemistry and Biophysics, University of Pennsylvania, Philadelphia, Pennsylvania, USA. [3]Neuroprotection Research Laboratory, Departments of Radiology and Neurology, Massachusetts General Hospital and Harvard Medical School, Charlestown, Massachusetts, USA. [4]Departments of Neurosciences and Radiology, University of California, San Diego, La Jolla, California, USA. Correspondence should be addressed to S.A.V. (vinograd@mail.med.upenn.edu) or D.A.B. (dboas@nmr.mgh.harvard.edu).

RECEIVED 3 DECEMBER 2009; ACCEPTED 6 JULY 2010; PUBLISHED ONLINE 8 AUGUST 2010; DOI:10.1038/NMETH.1490

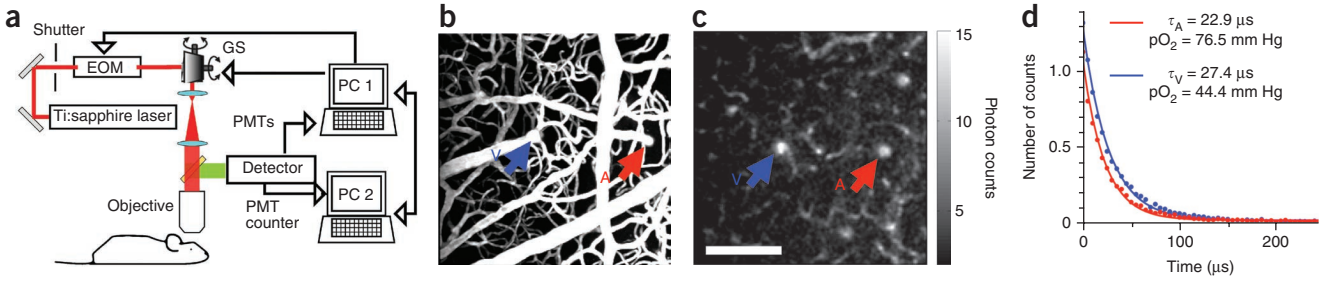

Figure 1 | Phosphorescence detection procedure. (**a**) Schematic of the experimental setup. EOM, electro-optic modulator; GS, galvanometer scanner. PMTs indicates analog-mode photomultiplier tubes, and PMT counter indicates a Geiger-mode photomultiplier tube. (**b**) Maximum intensity projection along the *z* direction of a 250-µm-thick stack in the mouse cortex. The vasculature was labeled with FITC. (**c**) Phosphorescence intensity image of microvasculature obtained at 166 µm depth below the cortical surface. The color bar shows the average number of photon counts in each pixel collected during a single phosphorescence decay. Scale bar, 100 µm. (**d**) Experimental measurement (dots) and corresponding single exponential fits (curves) of two phosphorescence decays from the diving arteriole (A) and ascending venule (V), with positions marked by the arrows in **b** and **c** to obtain the phosphorescence lifetime, τ.

coumarin-343 units, attached at the periphery of the dendrimer, capture two-photon excitation energy and transfer it nonradiatively to the porphyrin. Upon excitation, Pt porphyrin undergoes fast intersystem crossing into its triplet state and emits phosphorescence, which is quenched by molecular oxygen in a diffusion-controlled manner. Phosphorescence decay lifetime (typically several tens of microseconds) is inversely proportional to pO_2 (via Stern-Volmer relationship), thus forming the signal for analytical pO_2 determination.

The remaining termini on the dendrimer in PtP-C343 are modified with polyethylene glycol (PEG) residues. PEGylation ensures that the probe's signal is insensitive to proteins and other macromolecular solutes in biological systems. Dendritic porphyrin-based dyes used earlier could operate only when bound to albumin in the blood. However, at higher concentrations (above ~10^{-5} M), a substantial amount of these probes remain unbound, causing phosphorescence decays to become poorly interpretable, and pO_2 measurements irreproducible and inaccurate. PEGylated probes do not require binding to albumin for measurements in the physiological oxygen range and, if required, can be used at very high concentrations without causing ambiguity in pO_2 determination. In this study, we modified the probe with PEG residues of average molecular weight 2,000, as opposed to shorter PEG molecules (average molecular weight, 750), used in the original molecule[25]. This rendered the probe less aggregated and increased its signal dynamic range.

Experimental setup

For two-photon *in vivo* brain imaging, we constructed a microscope with high signal collection efficiency and photon-counting detection (**Fig. 1**). We imaged brains of anesthetized mice and rats through sealed cranial windows, either injecting the phosphorescence probe into the vasculature through the femoral artery or pressure-injecting it directly into the brain tissue. We obtained structural images of the cortical vasculature by imaging intravenously administered fluorescein isothiocyanate (FITC) conjugated with dextran. We excited phosphorescence by trains of femtosecond pulses from a Ti:sapphire oscillator, gated by an electro-optic modulator, and acquired decays by averaging multiple excitation cycles. Each cycle consisted of a 20–80-µs excitation gate, followed by 300-µs collection period, using an average laser power during the excitation gate of ~10 mW at the laser focus. We estimate that under this excitation regime the emitting volume had ~2 µm lateral (*x*-*y*) and ~5 µm axial (*z*) dimensions. This increase in the excitation volume, compared to its true diffraction-limited size, was caused by saturation effects[25]. Nevertheless, these dimensions still permitted sufficient spatial resolution and allowed for a much stronger signal and therefore a faster temporal response.

In a typical experiment, we performed detection in two steps. First, we raster-scanned the excitation beam over the field of view, rendering two-dimensional survey maps of the integrated emission intensity (250 × 250 pixels, acquired in ~25 s). A single-plane scan performed 166 µm below the brain surface (**Fig. 1c**) confirmed the ability of the system to resolve the structure of the microvasculature down to the capillary level. After mapping the tissue, we averaged 500–2,000 phosphorescence decays in selected locations in the vasculature for accurate pO_2 determination (**Fig. 1d**). This acquisition time corresponded to a temporal resolution of 0.16–0.76 s per single-point pO_2 measurement, whereas the measurement of the entire vasculature stack required up to 30 min. Finally, using Stern-Volmer calibration plots, we converted phosphorescence lifetimes, obtained by fitting, into pO_2 values.

Oxygen tension in cortical microvasculature

In a typical experiment we measured approximately 100 pO_2 values in 30-µm steps down to 240 µm below the cortical surface in the mouse brain (**Fig. 2a**). The obtained pO_2 values agreed well with previously published measurements in rat cortices[5,7]. We directly measured pO_2 in capillaries (**Fig. 2b** and **Supplementary Fig. 2**) and in consecutive vascular branches. Starting from the pial arteriole (**Fig. 2b**), pO_2 values changed from 61.1 mm Hg to 61.8 mm Hg, 48.2 mm Hg, 42.8 mm Hg and 29.7 mm Hg along the descending vessels down to the capillary level, at a depth of 240 µm.

We generally observed a decrease in the vascular pO_2 with an increase in the cortical depth (**Fig. 2c**). The average pO_2 (measured in three mice; excluding pial arterioles) decreased by ~10 mm Hg moving from the pial veins down to a depth of ~240 µm. This observation supported previous findings[6,27] that had showed a relatively rapid initial decrease of tissue pO_2 with increasing cortical depth. We also observed an average pO_2 increase of ~7 mm Hg toward the cortical surface in the three ascending venules (**Fig. 2c**) that drain blood from the deeper cortical layers, suggesting the possibility of oxygen efflux from

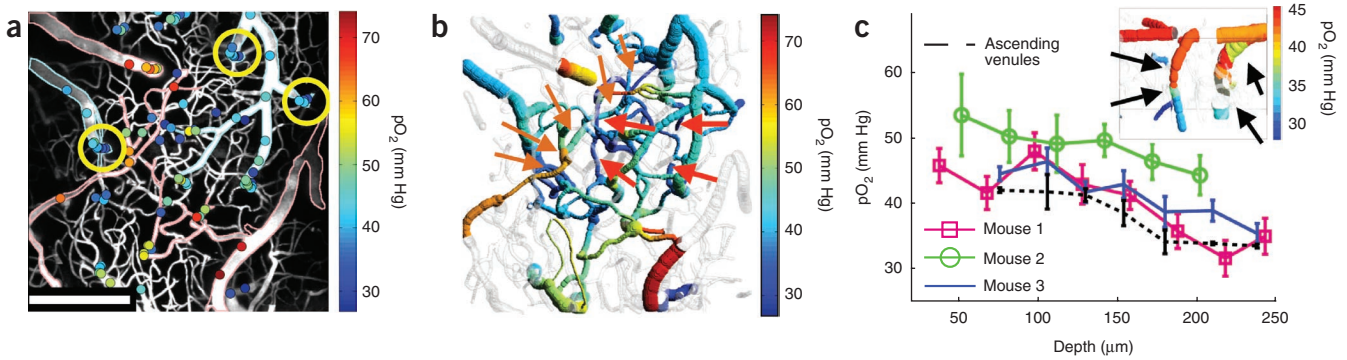

Figure 2 | Measurement of pO_2 in cortical microvasculature. (**a**) Measured pO_2 values in microvasculature at various depths (colored dots), overlaid on the maximum intensity projection image of vasculature structure (grayscale). Digital processing was performed to remove images of the dura vessels. Edges of the major pial arterioles and venules are outlined in red and blue, respectively. Scale bar, 200 μm. (**b**) Composite image showing a projection of the imaged vasculature stack. Red arrows mark pO_2 measurement locations in the capillary vessels at 240 μm depth. Orange arrows point to the consecutive branches of the vascular tree, from pial arteriole (bottom left arrow) to the capillary and then to the connection with ascending venule (top right arrow). Scale bar, 200 μm. (**c**) pO_2 dependence with cortical depth in three mice averaged across all vessels excluding pial arterioles. Dotted black line shows average pO_2 dependence with cortical depth in three ascending venules, at positions outlined with the circles in **a**. Error bars, s.e.m. Inset, composite image of the vascular structure and vascular pO_2 showing a side projection of the two circled ascending venules (arrows) from the top right corner in **a**.

the tissue into the venous compartment. A recent report makes a similar observation using the measurement of hemoglobin saturation as a vascular pO_2 indicator[28].

Oxygen tension in cortical tissue and microvasculature

To measure tissue pO_2, we injected PtP-C343 directly into the interstitial space. Based on the phosphorescence intensity measurements, PtP-C343 concentration in the tissue in these experiments was comparable to or lower than that used in vascular measurements. Two-photon excitation made it possible to confine the phosphorescence quenching by oxygen to the immediate vicinity of the focal plane, thus minimizing oxygen consumption and/or phototoxicity. Other studies have shown that oxygen consumption can skew tissue pO_2 measurements at high excitation intensities[21]. In our experiments, we could not observe any changes in the phosphorescence lifetime when performing multiple repetitive measurements at the same location.

We measured tissue pO_2 values (**Fig. 3**) during normoxia in a rat in 29 locations ~100 μm below the cortical surface (**Fig. 3c**). The obtained values (6–25 mm Hg) were within the range of the previously established cortical tissue pO_2 levels[5–7]. We observed relatively high pO_2 values (>20 mm Hg) close to a large pial artery and a relatively steep pO_2 decay at locations farther away from the artery. These results are in agreement with the existence of tissue pO_2 gradients at the cortical surface[5–7].

Two-photon phosphorescence lifetime measurements have the unique capability of simultaneously monitoring tissue pO_2 at multiple locations at variable depths, making it possible to conduct functional studies of the brain during transient changes in oxygenation. We acquired temporal pO_2 profiles at selected locations (**Fig. 3b**) during hypoxia, created by 30-s respiratory arrest (**Fig. 3d–f**). We averaged 500 decays in each location every 8.2 s, requiring 0.19 s per measurement, and we cycled the scan sequence for the duration of the experiment through all selected locations. We grouped the locations according to their distances from the artery. During hypoxia, oxygen rapidly depleted in all of the measured locations; however, we observed a clear correlation between the locations and the shape of the temporal profiles. Thus, closer to the artery (**Fig. 3e**) pO_2 decreased more slowly and recovered more quickly upon return to normal breathing, whereas in most locations farther away from the artery (**Fig. 3d,f**), pO_2 decreased faster and recovered more slowly.

To measure pO_2 concurrently in the vasculature and the interstitial space, we introduced PtP-C343 into both of these

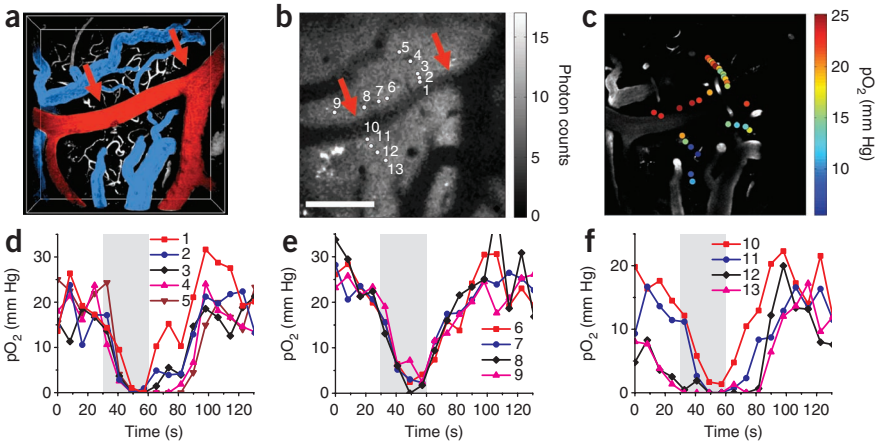

Figure 3 | Measurement of pO_2 in cortical tissue. (**a**) Volumetric image of the 200-μm-thick FITC-labeled microvasculature stack in the rat cortex. A large pial artery (red, arrows) and two pial veins (blue) are color-coded for easier identification. (**b**) An integrated phosphorescence intensity image at 100 μm depth. Arrows mark pial artery. Grey bar represents average number of counts from single phosphorescence decay at each pixel. Scale bar, 200 μm. (**c**) Measured pO_2 values during normoxia (colored dots), overlaid with a grayscale microvasculature structural image at 100 μm depth. (**d–f**) Temporal profiles of the measured pO_2 values at selected locations (labeled white dots in **b**) during hypoxia. Gray shading indicates the period of hypoxia.

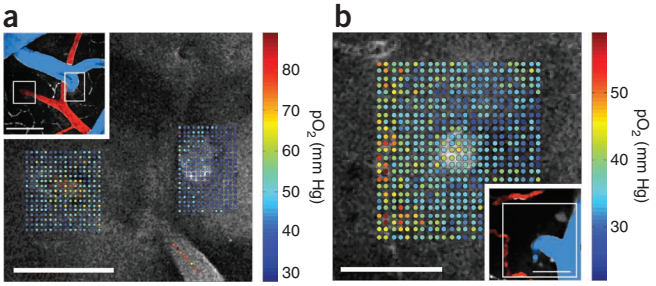

Figure 4 | Simultaneous measurement of pO_2 in cortical vasculature and tissue. (**a**,**b**) Measured pO_2 values (color bar scale) overlaid with the grayscale phosphorescence intensity image at 40 µm depth (**a**) and at 60 µm depth (**b**). In **a**, measurements were performed at locations of a descending arteriole (left) and an ascending venule (right). In **b**, measurements were performed at the location of an ascending venule. Insets, maximum intensity projections of 80-µm-thick FITC-labeled microvasculature stack with locations of pO_2 measurements boxed (artery and arteriole, red; vein and venule, blue). Scale bars, 100 µm (**a**) and 50 µm (**b**).

compartments. We obtained maps of pO_2 values measured at several locations around and inside diving venules and ascending arterioles in the rat cortex (**Fig. 4**). A map of more than 500 locations showed high pO_2 values inside and elevated pO_2 values around the diving arteriole (**Fig. 4a**). In contrast, we observed only slightly elevated intravascular pO_2 in the ascending venule with respect to the surrounding tissue pO_2. In a grid of pO_2 measurements, covering the area of an ascending venule and branches of a small descending arteriole, slightly higher pO_2 values were evident in the venule with respect to the surrounding tissue pO_2 (**Fig. 4b**). In addition, we noted elevated tissue pO_2 in the vicinity of the arterial branches.

DISCUSSION

With respect to brain studies, the key advantages of the two-photon phosphorescence quenching technique are its minimal invasiveness and the possibility of achieving high temporal and spatial resolution at substantial cortical depths. The probe's signal is independent of pH throughout the physiological range and is not affected by the presence of biological macromolecules[25]. Owing to its relatively large molecular size (~3–4 nm in the folded state), PtP-C343 is characterized by a long half life (~2 h) in the circulation (**Supplementary Fig. 3**). We did not detect any leakage of the probe from the vasculature into the interstitial space in the brain. A convenient feature of the method is its absolute calibration, that is, the probe constants need to be measured only once and do not require repetitive calibrations. Moreover, because the quenching reaction is independent of the pathway by which the probe is converted to its triplet state, we expect calibration plots (phosphorescence lifetime (τ) dependence on pO_2) to be identical for single- and two-photon excitation. Indeed, calibration of PtP-C343 confirmed that with a properly selected excitation regime, Stern-Volmer plots obtained *in vivo* in the blood using the two-photon microscopy setup were the same as those measured in a regular titration experiment using linear excitation (Online Methods and **Supplementary Figs. 1** and **3**).

It is important to keep in mind that in all quenching-based oximetry methods most of the photodamage occurs owing to the products of the quenching reaction (singlet oxygen and other reactive oxygen species). Thus, it is necessary to optimize probe concentration and excitation regime to minimize undesirable phototoxic effects. Two-photon excitation makes it possible to avoid formation of toxic species everywhere along the excitation path, and to confine it to the immediate vicinity of the laser focus. As a result, singlet oxygen generation in our experiments was minimized. We tested cell viability using apoptosis- and neuronal degeneration–sensitive staining 24 h after measuring tissue pO_2 in a dense grid pattern (**Supplementary Fig. 4**). In all cases, we saw no evidence of phototoxicity.

Until now, the lack of technologies for direct three-dimensional mapping of oxygen availability in the brain has been a major limiting factor in investigations of oxygen metabolism. Simultaneous imaging of intravascular pO_2 and tissue pO_2 gradients will allow direct measurement of oxygen extraction fraction and, when combined with measures of blood flow[29], the cerebral metabolic rate of oxygen, the central parameters for interpretation of blood oxygenation level–dependent functional magnetic resonance imaging fMRI[1]. Furthermore, our methodology for measuring pO_2 can be directly applied in other areas, such as stroke, cancer, neurological conditions and heart failure, where accurate noninvasive determination of pO_2 is key to understanding physiological function. The synergism of two-photon phosphorescent measurements with other two-photon microscopy tools for imaging of neuronal, vascular and metabolic activity opens the door to a more integrative approach for addressing critical questions regarding the order of pathological events in the progression of disease and promises to provide an objective way to screen potential therapies.

METHODS

Methods and any associated references are available in the online version of the paper at http://www.nature.com/naturemethods/.

Note: Supplementary information is available on the Nature Methods website.

ACKNOWLEDGMENTS

We thank W. Wu for performing the rat surgery, C. Ayata and G. Boas for critically reading the manuscript and support from US National Institutes of Health grants R01NS057476, P50NS010828, P01NS055104, R01EB000790, K99NS067050, R01HL081273 and R01EB007279 and American Heart Association grant 0855772D.

AUTHOR CONTRIBUTIONS

S.S., M.A.Y. and V.J.S. designed the microscope. E.R. synthesized the probe. S.S., M.A.Y., E.T.M., A.D., K.A. and S.R. performed experiments. S.S., D.A.B. and S.A.V. analyzed the data. D.A.B., S.A.V., E.H.L., S.S. and A.D. conceptualized and directed the research project. All authors discussed the results and commented on the manuscript.

COMPETING FINANCIAL INTERESTS

The authors declare no competing financial interests.

Published online at http://www.nature.com/naturemethods/.
Reprints and permissions information is available online at http://npg.nature.com/reprintsandpermissions/.

1. Heeger, D.J. & Ress, D. What does fMRI tell us about neuronal activity? *Nat. Rev. Neurosci.* **3**, 142–151 (2002).
2. Iadecola, C. Neurovascular regulation in the normal brain and in Alzheimer's disease. *Nat. Rev. Neurosci.* **5**, 347–360 (2004).
3. Takano, T. *et al.* Cortical spreading depression causes and coincides with tissue hypoxia. *Nat. Neurosci.* **10**, 754–762 (2007).
4. Erecinska, M. & Silver, I.A. Tissue oxygen tension and brain sensitivity to hypoxia. *Respir. Physiol.* **128**, 263–276 (2001).
5. Vovenko, E. Distribution of oxygen tension on the surface of arterioles, capillaries and venules of brain cortex and in tissue in normoxia: an experimental study on rats. *Pflugers Arch.* **437**, 617–623 (1999).

6. Masamoto, K., Takizawa, N., Kobayashi, H., Oka, K. & Tanishita, K. Dual responses of tissue partial pressure of oxygen after functional stimulation in rat somatosensory cortex. *Brain Res.* **979**, 104–113 (2003).
7. Sharan, M., Vovenko, E.P., Vadapalli, A., Popel, A.S. & Pittman, R.N. Experimental and theoretical studies of oxygen gradients in rat pial microvessels. *J. Cereb. Blood Flow Metab.* **28**, 1597–1604 (2008).
8. Gordon, G.R., Choi, H.B., Rungta, R.L., Ellis-Davies, G.C. & MacVicar, B.A. Brain metabolism dictates the polarity of astrocyte control over arterioles. *Nature* **456**, 745–749 (2008).
9. Koch, C.J. Measurement of absolute oxygen levels in cells and tissues using oxygen sensors and 2-nitroimidazole EF5. *Methods Enzymol.* **352**, 3–31 (2002).
10. Krishna, M.C. *et al.* Overhauser enhanced magnetic resonance imaging for tumor oximetry: coregistration of tumor anatomy and tissue oxygen concentration. *Proc. Natl. Acad. Sci. USA* **99**, 2216–2221 (2002).
11. Swartz, H.M. & Clarkson, R.B. The measurement of oxygen *in vivo* using EPR techniques. *Phys. Med. Biol.* **43**, 1957–1975 (1998).
12. Vanzetta, I. & Grinvald, A. Increased cortical oxidative metabolism due to sensory stimulation: implications for functional brain imaging. *Science* **286**, 1555–1558 (1999).
13. Wang, L.V. Multiscale photoacoustic microscopy and computed tomography. *Nat. Photonics* **3**, 503–509 (2009).
14. Fu, D., Matthews, T.E., Ye, T., Piletic, I.R. & Warren, W.S. Label-free *in vivo* optical imaging of microvasculature and oxygenation level. *J. Biomed. Opt.* **13**, 040503 (2008).
15. Vanderkooi, J.M., Maniara, G., Green, T.J. & Wilson, D.F. An optical method for measurement of dioxygen concentration based upon quenching of phosphorescence. *J. Biol. Chem.* **262**, 5476–5482 (1987).
16. Mik, E.G., Johannes, T. & Ince, C. Monitoring of renal venous pO_2 and kidney oxygen consumption in rats by a near-infrared phosphorescence lifetime technique. *Am. J. Physiol. Renal Physiol.* **294**, F676–F681 (2008).
17. Torres Filho, I.P. & Intaglietta, M. Microvessel pO_2 measurements by phosphorescence decay method. *Am. J. Physiol.* **265**, H1434–H1438 (1993).
18. Ances, B.M., Wilson, D.F., Greenberg, J.H. & Detre, J.A. Dynamic changes in cerebral blood flow, O_2 tension, and calculated cerebral metabolic rate of O_2 during functional activation using oxygen phosphorescence quenching. *J. Cereb. Blood Flow Metab.* **21**, 511–516 (2001).
19. Pastuszko, A. *et al.* Effects of graded levels of tissue oxygen pressure on dopamine metabolism in the striatum of newborn piglets. *J. Neurochem.* **60**, 161–166 (1993).
20. Shonat, R.D., Wachman, E.S., Niu, W., Koretsky, A.P. & Farkas, D.L. Near-simultaneous hemoglobin saturation and oxygen tension maps in mouse brain using an AOTF microscope. *Biophys. J.* **73**, 1223–1231 (1997).
21. Golub, A.S. & Pittman, R.N. pO_2 measurements in the microcirculation using phosphorescence quenching microscopy at high magnification. *Am. J. Physiol. Heart Circ. Physiol.* **294**, H2905–H2916 (2008).
22. Denk, W., Strickler, J.H. & Webb, W.W. Two-photon laser scanning fluorescence microscopy. *Science* **248**, 73–76 (1990).
23. Estrada, A.D., Ponticorvo, A., Ford, T.N. & Dunn, A.K. Microvascular oxygen quantification using two-photon microscopy. *Opt. Lett.* **33**, 1038–1040 (2008).
24. Mik, E.G., van Leeuwen, T.G., Raat, N.J. & Ince, C. Quantitative determination of localized tissue oxygen concentration *in vivo* by two-photon excitation phosphorescence lifetime measurements. *J. Appl. Physiol.* **97**, 1962–1969 (2004).
25. Finikova, O.S. *et al.* Oxygen microscopy by two-photon-excited phosphorescence. *ChemPhysChem* **9**, 1673–1679 (2008).
26. Lebedev, A.Y. *et al.* Dendritic phosphorescent probes for oxygen imaging in biological systems. *ACS Appl. Mater. Interfaces* **1**, 1292–1304 (2009).
27. Padnick, L.B., Linsenmeier, R.A. & Goldstick, T.K. Oxygenation of the cat primary visual cortex. *J. Appl. Physiol.* **86**, 1490–1496 (1999).
28. Hu, S., Maslov, K., Tsytsarev, V. & Wang, L.V. Functional transcranial brain imaging by optical-resolution photoacoustic microscopy. *J. Biomed. Opt.* **14**, 040503 (2009).
29. Srinivasan, V.J. *et al.* Depth-resolved microscopy of cortical hemodynamics with optical coherence tomography. *Opt. Lett.* **34**, 3086–3088 (2009).

ONLINE METHODS

Imaging setup. We used a custom-built microscope setup in this study (**Fig. 1a**). The system was controlled by custom-designed software written in LabView (National Instruments). The optical beam was scanned in the *x-y* plane by galvanometer scanners (6215H, Cambridge Technology, Inc.) and focused on the sample by an objective (Olympus 20X XLumPlanFL; numerical aperture (NA) 0.95). A motorized stage controlled the focal position along the vertical axis (*z*), and an electro-optic modulator (ConOptics, Inc.; extinction ratio ~500) served to gate the output of a Ti:sapphire oscillator (840 nm, 80 MHz, 110 fs, Mai-Tai, Spectra-Physics). The maximal laser power on the object during excitation gate was ~90 mW when imaging at large cortical depths and 10–20 mW at the surface. Increases in the power were necessary when working at higher depth to compensate for scattering and to maintain approximately 10 mW power in the focal plane. The pulse duration was ~350 fs (assuming sech2 pulse shape), as measured at the sample. The emission was reflected by a dichroic mirror (LP 735 nm; Semrock) and detected by a detector array, consisting of four independent photomultiplier tubes (PMTs), with a large collection efficiency (~15 mm^2 sr). The phosphorescence output was passed through a 680 ± 30 nm bandpass filter and forwarded to a photon-counting PMT module (H10770PA-50; Hamamatsu), whose output was acquired by a 50 MHz digital board (NI PCIe-6537; National Instruments) and saved for later processing. To determine the phosphorescence lifetime, we fitted the phosphorescence intensity decay with a single-exponential function using the nonlinear least-squares method. The lifetime was converted to pO_2 using the calibration plot obtained in independent oxygen titration experiments[25] (**Supplementary Fig. 3**).

Animal preparation. For imaging of pO_2 in the microvasculature, we anesthetized CD-1 mice (male, 25–30 g, 10–12 weeks old) by isoflurane (1–2% in a mixture of O_2 and N_2O) under constant temperature (37 °C). We then opened a cranial window in the parietal bone with intact dura and sealed it with a 150-µm-thick microscope coverslip. During the experiments, we used a catheter in the femoral artery to monitor the blood pressure (75–85 mm Hg) and blood gases (pCO_2, 36-39 mm Hg and pO_2, 110–160 mm Hg) and to administer the dyes. The concentration of PtP-C343 in the blood immediately after administration was ~16 µM. During the measurement period mice breathed a mixture of O_2 and air under the same isoflurane anesthesia.

For measurements of pO_2 in tissue (interstitial space), Sprague Dawley rats (250–320 g) were temperature controlled, anesthetized with isofluorane (1.5–2% in a mixture of O_2 and air) and tracheotomized, and catheters were inserted in the femoral artery and vein for administering the anesthesia and dyes and for measuring blood gases and blood pressure. We created a sealed cranial window in the center of the parietal bone with the dura removed. Before sealing the window, we pressure-injected ~0.1 µl of PtP-C343 (1.4×10^{-4} M) with a micropipette ~300 µm below the surface of the brain. We imaged a few hundred micrometers from the injection site. Probe spreading in the brain tissue was sufficiently slow to allow imaging of pO_2 for several hours after the injection. During the measurements, we ventilated rats with a mixture of air and O_2. Isofluorane was discontinued, and anesthesia was maintained with a 50 mg kg^{-1} intravenous bolus of alpha-chloralose followed by continuous intravenous infusion at 40 mg kg^{-1} h^{-1}. In the resting condition, the systemic arterial blood pressure was 95–110 mm Hg, pCO_2 was 35–44 mm Hg, and pO_2 was 95–110 mm Hg. We created hypoxic conditions by stopping the respirator for 30 s. We administered intravenous bolus of pancuronium bromide (2 mg kg^{-1}) followed by continuous intravenous infusion at 2 mg kg^{-1} h^{-1} during the breath-hold experiment to minimize possible animal motion. In all measurements, we compared the phosphorescence survey scans taken immediately before and after pO_2 point measurements and inspected collected phosphorescence decays for signs of sudden intensity or decay slope change during acquisition, which could indicate motion artefact during the measurement. For simultaneous intravascular and tissue pO_2 measurements, we used Sprague Dawley rats (90–120 g, 7 rats), applying the same surgical procedure. We adjusted intravascular concentration of the probe (10–30 µM) in each rat to obtain satisfactory visibility in phosphorescence survey images. Although preparations with tracheotomized rats allow generally longer and better controlled experiments, our choice of mice and small rats was motivated by a need to limit the amount of probe used in the experiments involving intravascular pO_2 measurements. All experimental procedures were approved by the Massachusetts General Hospital Subcommittee on Research Animal Care.

Construction of composite images. We obtained structural images of the cortical vasculature after collecting the pO_2 measurements by labeling the blood plasma with dextran-conjugated fluorescein (FITC; Sigma) and performing two-photon fluorescence imaging. We subsequently created a graph of the vascular network using a previously established procedure[30]. We performed image processing and data analysis using custom-designed software in Matlab (MathWorks); code is available from the authors upon request. The locations of the oxygen tension measurements were registered with this image, and three-dimensional composite images were created with both vasculature structure (grayscale) and color-coded measured pO_2 values. We color-coded the latter by assigning a pO_2 value either to the whole vessel segment between two branching points or to a neighboring portion of the vessel segment if more than one pO_2 measurement was performed in that segment. In addition, in some cases (**Fig. 2b**), for segments that did not have a measurement but joined at both ends with segments that had measurements within 100 µm, we assigned the average pO_2 value of the connecting segments. Although not quantitative, this procedure allowed more complete visualization of the vascular tree. In the future, simultaneous measurement of pO_2 and blood flow in the microvasculature[29] will greatly improve the accuracy of pO_2 estimation in the remaining parts of the vascular tree.

PtP-C343 synthesis and spectroscopy. We obtained all solvents and reagents from commercial sources and used them as received. We obtained PEG-amine of average molecular weight (MW) 2,000 from Laysan Bio. Inc. We synthesized PtP-$(AG^3OH)_4(C343)_5$ as described previously[25,31]. We performed preparative size-exclusion chromatography on S-X1 (Biorad) beads, using tetrahydrofuran (THF) as a mobile phase. The system for oxygen titrations was described previously[32,33]. We performed time-resolved phosphorescence measurements using a phosphorometer constructed in-house[34], modified for time-domain operation.

doi:10.1038/nmeth.1490

Synthesis of PtP-C343 modified with PEG-amines. Carboxy-terminated porphyrin-dendrimer $PtP(AG^3OH)_4(C343)_5$ (107 mg, 0.012 mmol) was dissolved in 10 ml of DMF. We heated the mixture for several minutes (~5–10 min) with a heat gun in the dark under argon flow and then allowed it to cool down to the room temperature (22 °C). Stirring continued until the dendrimer appeared fully dissolved. We added HBTU (2-(1H-benzotriazol-1-yl)-1,1,3,3-tetramethyluronium hexafluorophosphate) (182 mg, 0.48 mmol) in one portion and stirred the mixture for 5 min. We added DIPEA (N,N-diisopropylethylamine) (0.146 ml, 0.84 mmol) in one portion by a syringe, immediately followed by the addition of mPEG-NH_2, average MW 2,000 (960 mg, 0.48 mmol) in DMF (5 ml). The mixture was protected from ambient light and left stirring for 2 d.

We added ~30 ml of ether to the reaction mixture, leading to the formation of brightly colored oil while leaving the mother liquor colorless. The oil was separated by centrifugation, dissolved in THF, separated again by the addition of ether and centrifugation. This procedure was repeated two more times to remove most of the unreacted amino-PEG. We achieved the final purification by size-exclusion chromatography using THF as a solvent. The brown band was collected, the solvent was removed by rotary evaporation and the probe was briefly dried in vacuum. We dissolved this in a small amount of distilled water (~5 ml), filtered it through a polytetrafluoroethylene (PTFE) syringe filter (0.2 μm pore diameter) and freeze-dried it on a lyophilizer. The probe was isolated as brown solid material (yield, 86%).

30. Fang, Q. *et al.* Oxygen advection and diffusion in a three-dimensional vascular anatomical network. *Opt. Express* **16**, 17530–17541 (2008).
31. Lebedev, A.Y., Troxler, T. & Vinogradov, S.A. Design of metalloporphyrin-based dendritic nanoprobes for two-photon microscopy of oxygen. *J. Porphyr. Phthalocyanines* **12**, 1261–1269 (2008).
32. Rozhkov, V., Wilson, D.F. & Vinogradov, S.A. Phosphorescent Pd porphyrin-dendrimers: tuning core accessibility by varying the hydrophobicity of the dendritic matrix. *Macromolecules* **35**, 1991–1993 (2002).
33. Khajehpour, M. *et al.* Accessibility of oxygen with respect to the heme pocket in horseradish peroxidase. *Proteins* **53**, 656–666 (2003).
34. Vinogradov, S.A., Fernandez-Searra, M.A., Dugan, B.W. & Wilson, D.F. Frequency domain instrument for measuring phosphorescence lifetime distributions in heterogeneous samples. *Rev. Sci. Instrum.* **72**, 3396–3406 (2001).